Int. J. Advanced Networking and Applications
Volume: 17 Issue: 04 Pages: 7008-7022 (2026) ISSN: 0975-0290
https://doi.org/10.35444/IJANA.2025.17403

Design, Simulation, and Optimization of Cavity Patch Antenna used in Next-Generation 5G Wireless Communication

Kalim Ullah
Department of Electrical Engineering, University of Engineering and Technology Peshawar (Bannu Campus), Pakistan
Email: uetpeshawar2k19@gmail.com
Wajid Khan
School of Electrical and Information Engineering, Tianjin University, Nankai District, Tianjin, 300110, China
Email: engrwajidkhan@tju.edu.cn
Abdul Aziz
School of Electrical and Information Engineering, Tianjin University, Nankai District, Tianjin, 300110, China
Email:abdulamiruet@gmail.com
Mubarak Zeb
Department of Electrical and Computer Engineering, International Islamic University, Islamabad, (IIUI), Pakistan
Email:mubarak.mzb@gmail.com
Muhammad Zain Yousaf
Center for Renewable Energy and Microgrids, Huanjiang Laboratory, Zhuji, Zhejiang, 311816, PR China;
Email: mzainy1@gmail.com
Muneera Altayeb
Faculty of Engineering, Hourani Center for Applied Scientific Research, Al-Ahliyya Amman University, Amman, Jordan;
Email: m.altayeb@ammanu.edu.jo
Viktoriia Bereznychenko
Department of Theoretical Electrical Engineering and Diagnostics of Electrical Equipment, Institute of Electrodynamics, National Academy of Sciences of Ukraine, Beresteyskiy, 56, Kyiv 03680, Ukraine
Email: vika.bereznichenko@i.ua

ABSTRACT

The paper presents a rational design, simulates, and evaluates the performance of a high-frequency cavity-backed patch antenna specifically formulated to operate in the next-generation 5G wireless communications system. The antenna structure is undertaken to achieve an inbuilt structural compact design as well as the electromagnetic compact design with a balanced radiating patch of precise symmetrical design that integrates the substrate integrated waveguide (SIW) cavity, hence rendering the structure of the antenna very effective in its functioning. This is built with an architecture of five stacking layers comprising two substrate layers as well as an SIW feed arrangement of lines that are significantly located in a proper position to provide an excellent impedance match effect. The specified antenna is very robust in its operation across the frequency range of 26 GHz to 32 GHz, and its optimum resonance frequency resides at 28 GHz; that is in line with the international assigned mmWave bands to be used in 5G. The electromagnetic analysis also reveals a high return loss value of -54.129dB and a bandwidth of 3.3989 GHz, with minimal signal loss and an increase in data rate, as confirmed by full-wave electromagnetic simulation. The design antenna achieves a simulated directivity of 7.703 dBi at 28 GHz with radiation efficiency of -1.082 dBi (78%) and total efficiency of -1.083 dBi (78%), indicating minimal ohmic and mismatch losses across the operational bandwidth. Compared to existing counterparts, the proposed antenna exhibits a compact and cost-effective design while supporting wideband operation, enhanced radiation characteristics across a broad spectrum, and a high level of integration. The suggested antenna is a suitable choice for base stations and user equipment in the new-generation 5G communication network due to its low-profile design, high-frequency selectivity, and matching circuit technologies incorporated into the planar design. Its manufacture and its work enhance its capacity to commercially and industrially invade the mushrooming ultra-fast mobile connection world.

Keywords - **5G wireless communication, substrate-integrated waveguide (SIW), high-frequency antenna design, impedance matching, low return loss, wide bandwidth, mmWave bands, electromagnetic simulation.**

Date of Submission: November 03, 2025 Date of Acceptance: December 19, 2025

1. INTRODUCTION

Mobile wireless communication has grown to the extent that it has transformed connectivity by enabling real-time data sharing and information access. Nevertheless, the existing 4G LTE network is struggling to keep pace with the growing demand for higher data rates, reduced latency, and improved user experience. This bandwidth limitation has motivated the adoption of fifth-generation (5G)

Volume: 17 Issue: 04 Pages: 7008-7022 (2025) ISSN: 0975-0290
DOI :

wireless systems, which utilize higher-frequency or millimeter-wave (mm-wave) bands, particularly the 28 GHz spectrum, to ensure ultra-fast data transmission and enable bandwidth-intensive applications.

Millimeter waves offer vast unused spectral resources (30 GHz to 300 GHz) compared with sub-6 GHz bands, corresponding to wavelengths between 10 mm and 1 mm. The 28 GHz band lies at the lower edge of the mm-wave spectrum; however, its propagation characteristics are comparable to those of higher mm-wave frequencies. Owing to favorable trade-offs across system design parameters, this band is considered critical for practical early 5G terrestrial deployment. Notably, it supports wide contiguous bandwidths (up to 1 GHz or more), enabling peak data rates exceeding 10 Gbps, which are suitable for applications such as ultra-high-definition video streaming, virtual reality, and autonomous vehicles. Additionally, the 28 GHz band facilitates spatial reuse, beamforming, and enhanced security, as it is compatible with compact, high-gain antenna arrays.

Irrespective of these advantages, mm-wave communication systems face significant challenges, particularly high free-space path loss. For instance, a 60 GHz signal experiences attenuation over 1 km comparable to that of a 600 MHz signal over 100 km. Atmospheric absorption and rain attenuation further complicate outdoor implementations, although rain attenuation is relatively weaker at 28 GHz (approximately 0.06 dB/km) compared to higher mm-wave frequencies. Consequently, advanced antenna designs play a vital role in mitigating these propagation impairments.

Microstrip patch antennas (MPAs) have become a fundamental component of modern wireless communication systems due to their numerous advantages, including low profile, lightweight structure, ease of integration with both planar and non-planar surfaces, and cost-effective manufacturing using printed circuit technology [1]. These characteristics make MPAs particularly attractive for mm-wave and 5G applications. However, conventional microstrip patch antennas suffer from narrow bandwidth and low gain, which limit their suitability for mm-wave communications.

Recent research efforts have focused on overcoming these limitations through innovative design techniques. Cavity-backed structures and substrate-integrated waveguide (SIW) technology have gained considerable attention due to their ability to suppress surface waves and enhance radiation efficiency and bandwidth. For example, the effectiveness of aperture-coupled patch antennas using SIW feeding [2] and LTCC-based multibeam arrays [3–4] has been demonstrated, although fabrication complexity remains a challenge. Wideband operation has also been achieved using alternative approaches, such as parasitic elements [5] and dual-resonant slot–patch designs [6], often at the expense of increased size or cost.

This paper extends these developments by proposing a cavity-backed microstrip patch antenna optimized for 5G systems operating at 28 GHz. The proposed configuration consists of a symmetrical patch and an SIW cavity incorporating split (modified) slots to enable quasi-TM02 mode operation. The antenna achieves an impedance bandwidth of 2.9 GHz and a return loss of −47 dB at the resonance frequency. Such performance is particularly critical for dense urban environments, where efficient and reliable 5G deployment is most essential.

The literature highlights the significance of mm-wave bands for 5G communication, with pioneering studies [3, 7] demonstrating the feasibility of high-throughput links. Propagation models for 28/38 GHz bands have informed system-level designs [8], while large-scale array prototypes have been investigated in [9]. Furthermore, [10] emphasized the role of massive MIMO and mm-wave spectrum in 5G architecture. Recent advancements in SIW-based patch antennas [11–12] and metallized cavity designs [13] have paved the way for high-gain and bandwidth-enhanced antennas. Building upon these insights, ongoing research continues to advance the development of compact and efficient antennas for next-generation wireless networks [14–15].

Table 1: Literature Review Summary

Ref	Methodology	Contributions	Limitations
[16]	Narrow-wall slot-fed SIW design	Improved bandwidth via narrow-wall slot feeding	Bulky size
[17]	Planar SIW backed slot antenna	Suppressed surface waves, wide impedance bandwidth	Limited compactness
[18]	High-order mode (HOM) cavity	Enhanced gain and bandwidth	Difficult design Tuning
[19]	Dual-mode cavity Slot	Simultaneous operation in dual bands	Moderate gain
[20]	Wide slot with cavity backing	Increased beam directivity	Complex to Fabricate
[21]	Integrated SIW-fed patch array	Full band mm Wave coverage	Increases thermal complexity
[22]	Dual-resonant cavity	Enhanced beam steering capability	Lower return loss
[23]	Wideband SIW rectangular patch	Stable directional gain	Poor polarization Control
[24]	Compact patch array via SIW	Manufactural and Broadband	Slight return loss Degradation
[25]	Aperture-fed cavity-backed patch	Superior matching and gain	Complex Fabrication
[26]	LTCC dielectric Integration	Stable dielectric response	Cost-intensive

Volume: 17 Issue: 04 Pages: 7008-7022 (2025) ISSN: 0975-0290
DOI :

[27]	LTCC dielectric integration	Stable dielectric response	Cost-intensive
[28]	Multilayered cavity Etching	Size reduction and high isolation	Poor integration flexibility
[29]	Dual-mode cavity Design	Supports dual polarization	Decoupling issues
[30]	Truncated cavity patch	Antenna size minimized	Side-lobe increase
[31]	Cavity E-patch for mm Wave	Balanced gain and directionality	Suboptimal axial ratio

The primary objective of this research is to design and optimize a high-performance microstrip patch antenna specifically tailored for 5G mm-wave applications, with a focus on the 28 GHz frequency band. The key design goals outlined for this study are as follows:

i. The antenna must support high data rate communication by providing a wide bandwidth, enabling seamless operation over a broad frequency range, thus accommodating the increased demands of 5G networks.
ii. A critical design requirement is achieving good impedance matching with a return loss (|S11|) of less than -10 dB. Through simulations, the antenna's performance is optimized to achieve a return loss of -54.129dB, ensuring minimal signal reflection and efficient power transfer.
iii. To offset the high path losses encountered at mm-wave frequencies, particularly at 28 GHz, the antenna's gain and radiation efficiency must be optimized to ensure reliable communication. even in environments with significant signal attenuation.
iv. The design aims to maintain a balance between performance and practical considerations. It is important to keep the antenna's structure simple and cost-effective, making it feasible for mass production and integration into real-world 5G systems.

To achieve these objectives, the research investigates various design parameters, including the dielectric constant of the substrate, substrate thickness, loss tangent, feed type, and patch geometry. The proposed antenna utilizes an innovative cavity-backed patch design, incorporating SIW cavity technology and modifications such as L-shaped and hammer-like slots to optimize the antenna's performance. Extensive simulations have been conducted to evaluate the antenna's performance metrics, such as return loss, bandwidth, Voltage Standing Wave Ratio (VSWR), radiation pattern, and efficiency. The antenna design has been fine-tuned to operate effectively within the 26–32 GHz band, with a particularly strong resonant response at the target frequency of 28 GHz, making it a promising candidate for 5G mm-wave communications.

2. METHODOLOGY AND PROJECT DEVELOPMENT

Microstrip patch antennas form an important part of modern communication systems that are usually preferred due to their low cost, miniaturized structure, and ease of fabrication. Their preference makes the antenna suitable for various other wireless applications, including mobile, satellite, and GPS. These antennas were initially designed in 1972 and fall within the microwave spectrum of frequencies. Since then, the antennas have been developed to fulfill the requirements of current wireless technologies. The common structure of a patch antenna in microstrips comprises a metallic shooting radiator patch, a dielectric substrate to support it, and the ground plane, and all these contribute to its functioning. The patch may be rectangular, circular, or L-shaped, among others, with each having different radiation patterns that are useful in specific applications. The size of the antenna and its capability to be combined with microwave circuits are especially desirable on smaller, portable devices and for array systems, which enhance radiation performance in more advanced systems, such as 5G and radar systems.
Although microstrip patch antennas are known to have numerous merits, such as ease of generation, low cost, and ease of integration, they also have their shortcomings. These antennas have low gain and limited bandwidth, which can restrict their use in long-range communication or high-power scenarios, unless special measures are taken.

Arrangements, such as stacked patches and cavity-backed structures, are applied. Moreover, the microstrip antennas exhibit rather poor radiation efficiency, especially at the higher frequencies, which is caused by material losses in the dielectric and, especially, the conductor. Microstrip antennas, despite these pitfalls, are still actively gaining popularity in various spheres due to their universality and affordability. They find use in mobile satellite communication systems, wireless LANs, GPS systems, and military technology, which demonstrates the significance of these devices in both civilian and military communication systems. Other important theories and works on this have been reported in the past; hence, these are the key references of our clear microstrip patch antenna. It is explained in great detail in earlier chapters. As a rule, this section will represent how the Design Cavity Patch Antenna could be applied to 5G Wireless Communication. The initial thing that needs to be known is all the main parameters of a Line Microstrip Patch Antenna.

The model on which our design is based is the CST software. CST Microwave Studio (CST MWS) is a highly specific program that can be used to simulate 3D electromagnetic (EM) behavior in high-frequency components. CST MWS offers a quick and precise simulation of high-frequency (HF) equipment of antennas, filters, couplers, flat, and multi-layered structures. The software is a facility that provides insight into the EM behavior of high-frequency designs, which CST MWS

Volume: 17 Issue: 04 Pages: 7008-7022 (2025) ISSN: 0975-0290
DOI :

offers in an easy-to-use software for this project. CST can be applied to model and solve radiation characteristics, S-parameters, 1D, 2D, and 3D solutions, as well as field monitors. The simulated results will then be compared, and it was found that different antennas have different simulated results. Our design strategy is summarized below by the following flow schema.

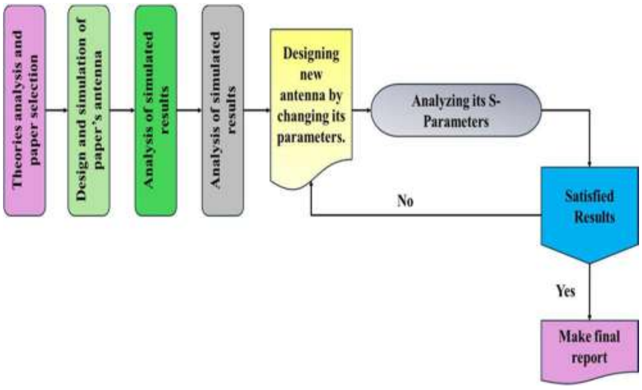

Figure 1: Research Framework Flowchart

3. DESIGN METHODOLOGY AND ANALYSIS

In designing a rectangular microstrip patch antenna, four essential parameters must be carefully considered to ensure optimal performance, especially for high-frequency applications like 5G communication systems. First, the operating frequency (f_o) plays a critical role, as it determines the resonant point of the antenna. For 5G applications, the 28 GHz band has emerged as one of the most promising candidates due to its wide bandwidth and favorable propagation characteristics, making it a suitable choice for high-speed and low-latency wireless systems [1–3]. Second, substrate dielectric constant (εr) also contributes greatly to the size and the performance of the antenna. For this design, Rogers RT5880 is a lossy dielectric material chosen due to its low loss tangent and high frequency stability. This substance facilitates effective signal transmission and helps to maintain the antenna in a compact size. Third, the dielectric substrate height (h) is a major parameter that determines low-profile design.

Because the 5G systems require small and lightweight equipment, the substrate height is 0.79 mm to maintain an antenna that is thin and able to integrate with other parts of the circuit. Fourth, the patch (t) height is kept so low to save even more of the overall antenna volume, which goes in the direction of reduced overall size of the devices, which is the design philosophy of the 5G era. In this work, the patch height is chosen as 0.035 mm, and this contributes to the slimness of the antenna. Other geometries, including the patch width (W), patch length (L), ground plane, and substrate width (W) and length (L), are well-considered parameters in calculations regarding the target frequency and the properties of the substrate, in addition to these fundamental parameters.

To analyze and optimize the performance of the microstrip patch antenna, certain working techniques are typically employed, which involve a variety of analytical and numerical methods. The Transmission Line Model provides a simplified analysis that facilitates basic comprehension and quick computations [3]. The use of the Cavity Model is more precise in the estimation of resonant modes and field distribution in the patch [4]. In more detailed simulations, the Method of Moments (MoM) [5] and the Finite-Difference Time-Domain (FDTD) method [6], which are more rigorous, may be used to approximate more complicated electromagnetic behavior and ensure that the antenna works properly over the desired frequency range. These methodologies can be utilized to facilitate the proper design and optimization of the next generation of high-performance antennas for wireless technology. The patch antenna is modelled as two parallel radiating slots with a transmission line in between in the transmission line model. The patch antenna length of the model is supposed to be larger than the physical length underlying the fringing effect at the edges of the patch. The transmission-line model is simple to apply, but it has certain drawbacks. It can only be used to rectangular (or square) shaped patches. It automatically disregards information of field variations at the radiating edges.

Some of the shortcomings associated with the Transmission Line Model have also been addressed through the use of the cavity model. Cavity-based calculations are the most valuable for studying patch antennas. The cavity model considers the area between the two parallel conductor planes comprising a patch radiator and ground plane as a cavity defined by electric walls and a magnetic wall on the periphery of the patch. Once the field distribution has been found on this cavity, the antenna fields are taken to be those of this cavity. Application of Huygens' Principle can be done to the magnetic wall of the cavity, and the approximate radiation field can be calculated. This is the best technique to be used when analyzing patch antennas whose geometry, as well as the wave equation that describes this geometry (cavity model), can be solved using the separation of variables method.

The configurations of rectangular microstrip patch antenna arrays have been studied with the use of an algorithm and software that uses the method of moments. The counts of input impedance, mutual integration, and radiation patterns are made, and the results are compared with an experimental mode. The process of the moment, in that it is less specific, though very computationally cumbersome, yields at least some physical understanding. The cavity model provides a simple as well as a physically insightful model [7]. In this Paper, the FDTD (Finite-difference Time-domain Method) method is applied, namely CST Microwave Studio FDTD software. The FDTD method uses finite element formulas (based on approximate differentials) to discretize Maxwell equations. Maxwell equations treat finite differences to spatial and time derivatives. The strengths of the FDTD method are: it is

Volume: 17 Issue: 04 Pages: 7008-7022 (2025) ISSN: 0975-0290
DOI :

possible to analyze arbitrarily shaped structures, and it covers a large range of materials that can be modeled. In FDTD, any volumetric cell can have its own permittivity, independent of all other cells. FDTD can be very convenient in the case of very broadband excitations, where the solutions are obtained at many frequencies through a single calculation in the time domain. The Fourier Transformation of a time-sampled scattered waveform gives the necessary parameters in a broad band.

CST Microwave Studio is a comprehensive parameter tool for creating quick and accurate EM, 3D simulations of high-frequency issues. It features full parameterization, including electrostatics and magneto statics solvers, as well as other important features such as VBA compatibility, automatic multi-dimensional sweeps, optimizers, and automatic macro recording. CST-based designing has also enabled the use of an interactive mouse to input data, capture designs, and assist with templates for particular applications, as well as complete parametric 3D modeling. The editing can be undone and redone with no limits on a history list. Elaborated solid modeling capabilities are also available through the software, and it includes helices, blends, chamfers, extrusions, lofting, and Boolean operations of adding and subtracting solid objects to existing constructions. It also enables the usage of imported 3D and planar structures, as well as the parameterization of the imported objects. The software has automatic meshing and adaptive mesh refinement. Simulation materials may be arranged in stacks, both isotropic and anisotropic, both linear and non-linear, magnetic and non-magnetic. Examples of RF energy excitation sources are waveguide ports, plane wave incident fields, and discrete voltage and current sources. Post-processing involves the VSWR and Smith chart predictors, port signal predictors, polar radiation pattern predictors, and planar and spatial grid field predictors. The software is also capable of calculating and plotting the antenna axial ratio, which is of importance to a circular and elliptically polarized antenna.

Designing an antenna begins with identifying the criteria to be adopted when choosing the best antenna. The initial requirement is that of transferring power between the feed transmission line and the antenna. This can be achieved by matching the input impedance of the antenna with the characteristic impedance of the transmission line. This time, a microstrip line is used, where the line characteristic impedance is 50 ohms. The above relationship is described as follows:

$$\Gamma = \frac{Z_L - 50}{Z_L + 50} = \frac{VSWR-1}{VSWR+1} \quad (1)$$

$$VSWR = \frac{1+\Gamma}{1-\Gamma} \quad (2)$$

$$\text{Mismatch Loss (dB)} = -\log_{10}[1 - \Gamma^2] \quad (3)$$

To achieve the minimum acceptable VSWR of 2:1, the reflection coefficient must be Γ = 0.333, a corresponding load impedance of ZL = 100Ω ohms and transmission line impedance of $Z0$ = 50Ω, where to attain the transmission line characteristic impedance of $Z0$ = 50Ω, and load impedance of ZL = 100Ω to arrive at a minimum acceptable VSWR ratio of 2:1, then the reflection coefficient would be Γ = 0.33

$$Z_L = (-50)\left(\frac{1+\Gamma}{1-\Gamma}\right) \quad (4)$$

The other critical requirement in choosing an antenna is its total efficiency, which is the product of the input efficiency, radiation efficiency, and the beam efficiency, and is formulated by the following relation:

$$\eta_{overall} = \eta_{input} . \eta_{rad.} \eta_{beam} \quad (5)$$

The efficiency is the fraction of input power effectively coupling the source power with the antenna, and it is calculated as follows:

$$\eta = 1 - |\Gamma|^2 \quad (6)$$

At this point, where the symbol 9 is the reflection coefficient or S_{11} as defined by:

$$\Gamma = \frac{Z_{in} - Z_{ref}}{Z_{in} + Z_{ref}} \quad (7)$$

CST Microwave Studio designates the reflection coefficient by the parameter S11. The radiation efficiency gives the factor of coupled power that radiates with an antenna, and it is presented in a ratio of the radiated power to the input. Mathematically it's given as:

$$\eta_{rad} = \frac{P_{rad}}{P_{in}} - \frac{R_{rad}}{R_{rad} + R_L} \quad (8)$$

Here, $Rrad$ is effective radiation resistance, and R L is antenna loss resistance. The antenna radiation efficiency is low when the radiation resistance is small in comparison with the loss resistance. In electrically small antennas the radiations resistance is proportional to $\frac{L^2}{\lambda}$ (an electrically small loop), and $\frac{L}{\lambda^4}$ (an electrically short dipole), where L is the length of the antenna, and lambda is the wavelength at the operating frequency.

In our proposed antenna, we initially produced a cavity patch antenna with a higher order of TM02 mode of patch antenna and substrate integrated waveguide (SIW) cavity. We then further changed the design where we injected the L-shaped structure at a diagonal direction, and symmetrical U-shaped structures with rectangular and hammer-shaped structures in the patch. The change enhanced the antenna bandwidth and reduced the return losses. Simple structure, good stability in gain, as well as, above all, ease of use are the intrinsic properties of the suggested antenna.

3.1 CAVITY PATCH ANTENNA

Figure 2 shows the 3D structure of a cavity patch antenna (Antenna-A), a top view of the patch of the antenna. Antennas contain two parts, i.e. a top patch and a bottom substrate integrated wave (SIW) cavity with a thin substrate between them. The cavity is shaped as SIW by using a pattern of

Volume: 17 Issue: 04 Pages: 7008-7022 (2025) ISSN: 0975-0290
DOI :

metallic via in a dielectric substrate of Rogers RT5880, which is 0.785mm thick, as shown in Table 1. An SIW cavity will allow mitigating the effects of the feeding technique on the antenna radiation pattern. To reduce the energy reflection on the side wall of the SIW cavity, the diameter (D) and the center-to-center distance (S lm) should satisfy the following condition $\frac{D}{\lambda_0} \geq 0.1$ and $\frac{D}{S_{lm}} \geq 0.5$ L n p and W np the length and width of the SIW cavity can be numerically. Calculated using the presented two equations:

$$L_{eqn} = L_{mnp} - \frac{D^2}{0.95 S_{lm}} \quad (10)$$

To justify the selection of the cavity model for the proposed antenna design, a comparative analysis with other commonly used modeling approaches is presented in Table 2.

Table 2: Cavity vs. Other Model

Aspect	**Cavity Model**	**Transmission line Model**	**Full-Wave (Numerical)**
Accuracy	High [32], [33]	Lowest	Most accurate [33]
Complexity	Moderate [34], [35]	Simplest [34]	Highly complex
Physical insight	Excellent [35]	Good	Low
Patch Shape	Applicable to regular shapes [32]	Strictly for rectangular patches [33]	Versatile

4. Simulation and Results

Table 7 presents a detailed performance comparison between the proposed model and existing reported model in terms of key parameters such as operating frequency, bandwidth, return loss, directivity, radiation efficiency, total efficiency, polarization, number of beams, and beam direction. The results of the simulated output of the proposed cavity-backed patch antenna were assessed comprehensively to assess further its applicability in the realm of millimeter-waves and in the frequency range of 28 GHz. The antenna features superior impedance matching, a broad bandwidth, and high efficiency. The S-parameter output S11 shows that there exists a deep resonance at about 28.04 GHz with the lowest value of -44.1218dB, which implies little signal reflection. To add to this, the VSWR values are near the optimum 1.00 as ideal, which is to certify that the impedance is matched optimally throughout the band. The design also exhibits stable output even with small parametric changes, further demonstrating its strength and reliability in high-frequency systems, such as 5G wireless systems.

4.1 For Antenna 01

Figure 2 represent the 3-dimensional construction of a cavity patch antenna 01, which has two planes consisting of a top patch and a substrate integrated wave (hybrid) cavity at the bottom, which are divided by a thin substrate plane. This antenna is suited for high-frequency applications, such as communication systems with 5G, due to its symmetrical structure, which provides adequate radiation and low cross-polarization.

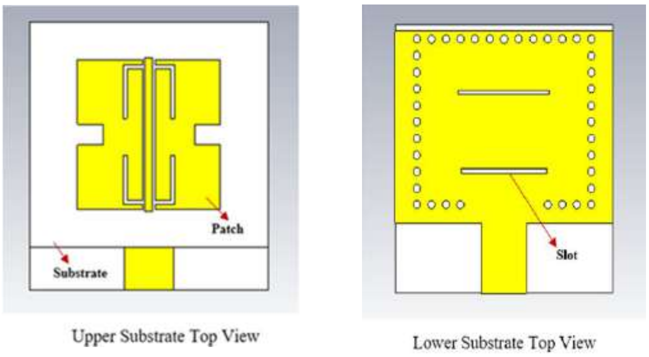

Figure 2: Beam cavity-backed patch antenna 01 structure

The return loss is one of the most important parameters to use in the initial phase of designing and analyzing a microstrip patch antenna. Return loss is the efficiency of the input power used by the antenna, and the lower the value of the return loss, the more efficient the power taken up by the antenna. The smaller the return loss, the greater the power radiated by the antenna, and vice versa, and the larger the values, the more the reflection of the signal, and the poorer the use of power. Figure 2 and picture 2 represent the 3-dimensional construction of a cavity patch antenna 01, which has two planes consisting of a top patch and a substrate integrated wave (hybrid) cavity at the bottom, which are divided by a thin substrate plane.

When the command of Parametric Sweep was used on "L1", the return loss value increased a lot. In Figure 11, the characteristics of S11 of Antenna 2 have been plotted in the frequency range of 26-32 GHz with various changes made in parameters. The plot shows clear and solid resonances at approximately 28.004 GHz, with a maximum negative return loss of 44.1218 dB, indicating good impedance matching and minimal reflection of any signal. These different traces have varying configurations, including parameter sweeps. Still, in each case, the return losses are kept below -30 dB at resonance, indicating the relative robustness and dimensional flexibility of the antenna. This overall performance essentially demonstrates the stability of the design and its compatibility with high-frequency (mm-wave) applications, as well as those requiring high reflectivity and high matching, such as 5G systems.

Volume: 17 Issue: 04 Pages: 7008-7022 (2025) ISSN: 0975-0290
DOI :

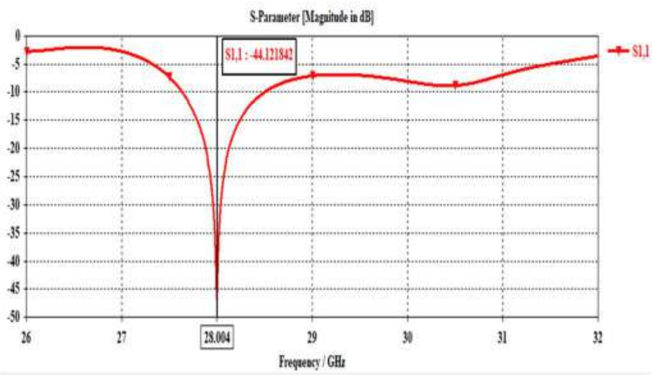

Figure 3: Graphical view of Return Loss of Antenna 01

Figure 4 shows a plot of return loss applied to achieve the impedance bandwidth of Antenna 01. An acceptable threshold is hereby established using a -10 dB threshold level and the frequencies at which the antenna transmits less than 10 percent of the signal incident upon it. And the antenna exhibits a return loss smaller than -10 dB across the range of approximately 27.638 GHz to 28.501 GHz; therefore, the bandwidth is 0.86271 GHz (or 862.71 MHz). This bandwidth is particularly convenient in the millimeter-wave field, especially at 28 GHz, which is being utilized in 5G networks. As a result, the performance is stable, and the band can accommodate a wide frequency range with reduced reflection, making signal transmission more effective.

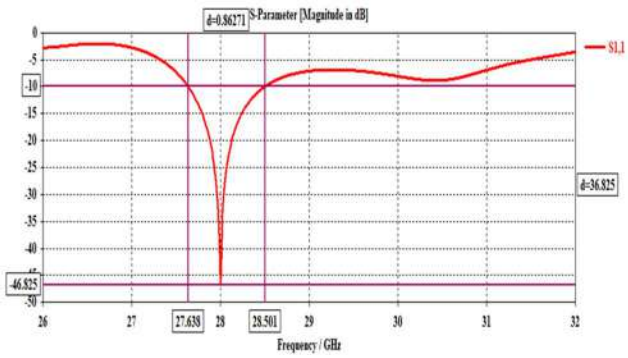

Figure 4: Antenna 01 Graphical Analysis of Bandwidth

Figure 5 illustrates the 3D gain radiation pattern of Antenna 01 at 28 GHz. The antenna has a gain of 6.838 dB, with the principal beam aligned along the positive z-axis, demonstrating pronounced directional radiation characteristics. The spherical plot shows an ideal main lobe with comparatively low side lobes, suggesting that undesirable radiation in off-axis directions is being highly suppressed. The radiation and total efficiencies are also noted as -1.353 dB and -1.432 dB, respectively, indicating a minimum loss of power in the antenna and demonstrating that the antenna can radiate effectively. This measurement suggests that, when applied to the 5G mm Wave type of service, Antenna 02's performance is ready to present mm Wave-related high-gain and narrow beams essential for sending reliable point-to-point communication.

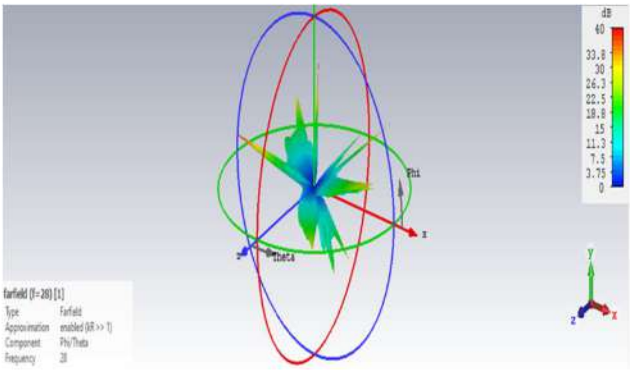

Figure 5: 2D Farfield Gain of Antenna 01

Figure 6 presents the polar diagram of the far-field gain of Antenna 01 at 28 GHz, Phi = 0 degrees plane. The principal lobe has a maximum increase of 7.38 dB, and its beam is skewed at an angle of -5.0°, which is not perpendicular to the boresight. It has a 3 dB angular width of 57.9°, which represents a fairly directional radiation pattern capable of simultaneous coverage and directionality. Furthermore, the side lobe level is -12.8 dB, indicating that off-axis radiation is effectively suppressed and poses a low threat of interference. Such radiation characteristics demonstrate that Antenna 02 is well-suited for millimeter-wave communications, offering not only significant gain but also directional control that necessitates the deployment of 5G systems.

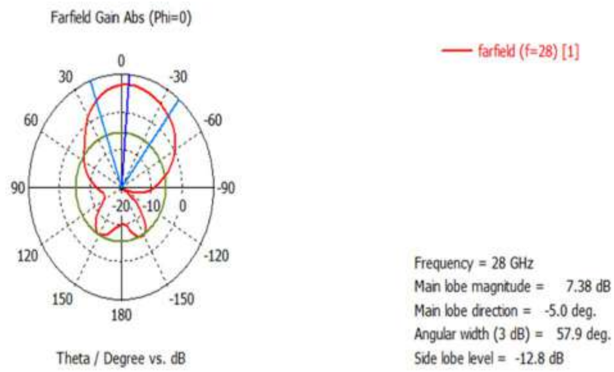

Figure 6: Polar Gain of Antenna 01

Figure 7 presents the 3D graphical view of Directivity of antenna 01. The antenna offers a high-end directivity of 8.865dBi, with the main radiation lobe directed along the positive z-axis, providing highly directional characteristics. The radiation pattern features a concentrated principal beam and well-managed side lobes, which are ideal for targeted applications of millimeter waves. The corresponding total efficiencies and radiations are -1.353dB (71.91%) and -1.432dB (73.23 %,), respectively, indicating that the antenna structure performs well in reducing power losses. The high directivity and effective radiation properties suggest that the antenna can be utilized in high-frequency applications, including but not limited to 5G beamforming, as well as other wireless communication systems that require specific, directed signal outputs.

Volume: 17 Issue: 04 Pages: 7008-7022 (2025) ISSN: 0975-0290
DOI :

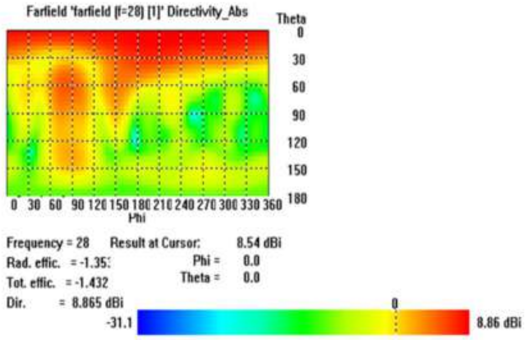

Figure 7: 3D Graphical View of Directivity of Antenna 01

The geometrical and material parameters for Antenna 01 are detailed in Table 3. The substrate of the antenna is of relative permittivity (2.2), height (0.79 mm), and width (13.56 mm), which results in low dielectric loss and allows it to be operated at high frequencies. Its layout has well-defined strapline and slot sizes, e.g., Trace Width = 2.8 mm, Wsiw = 9.6 mm, and Lsiw = 8 mm. It is possible to integrate substrate-integrated waveguide (SIW) structures to achieve guided-wave performance. The length L = 13 mm, width W = 10 mm, and other slot and patch dimensions are fine-tuned to resonate at 28 GHz, thereby achieving the desired impedance matching, gain, and bandwidth. This comprehensive design specification enables the successful operation of the antenna in the millimeter-wave range, including 5G and beyond.

Table 3: Antenna 01 Design Parameters

S.No.	***Antenna Parameters***	***Dimensions***
1	*Length of Lower substrate*	13mm
2	*Width of Lower substrate*	10mm
3	*Length of upper substrate*	112mm
4	*Thickness of substrate*	0.785mm
5	*Thickness of ground*	0.035mm
6	*Length of lower patch*	9mm
7	*Width of lower patch*	10mm
8	*Thickness of patch*	0.035mm
9	*Length of feed line*	3.4mm
10	*Width of feed line*	2.454mm
11	*Thickness of feed line*	0.035mm

4.2 FOR ANTENNA 02

Figure 8 presents the graphical representation of Antenna 02, depicting its geometry on the top layer. The structure consists of a symmetrical array of copper patches (shown in yellow) mounted on a dielectric substrate. The design features various rectangular and slot-like components, indicating a complex resonant structure designed to tune performance and increase bandwidth. The symmetrical nature of the layout also suggests the prospective dual-polarization or balanced feeding. This is generally optimized to operate in the millimeter-wave range and can be used in high-performance communication systems, such as in 5G and radar applications, where small size and high performance are required.

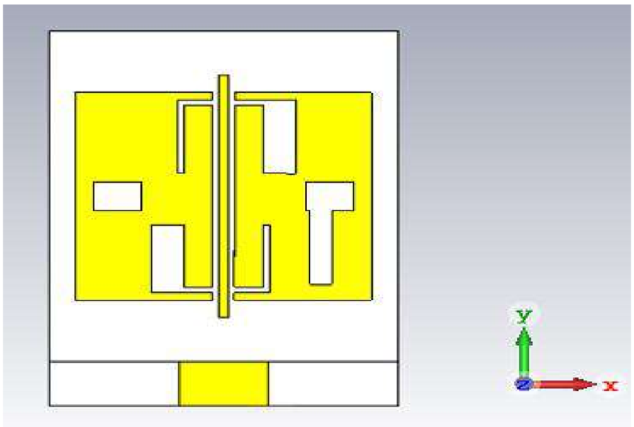

Figure 8: Graphical representation of Antenna 02

Figure 9 shows the S11 characteristics of Antenna 02 over the frequency range of 26–32 GHz. A pronounced resonance is observed at 28.07 GHz, where the return loss reaches a minimum value of –32.2122 dB. This deep null indicates excellent impedance matching and minimal signal reflection at the target frequency, which is critical for efficient power transfer in high-frequency applications. The return loss remains below –10 dB over a broad frequency span, suggesting a wide operational bandwidth. Such performance highlights Antenna 02's suitability for millimeter- wave systems, particularly in 5G communication, where low return loss and stable resonance around 28 GHz are essential.

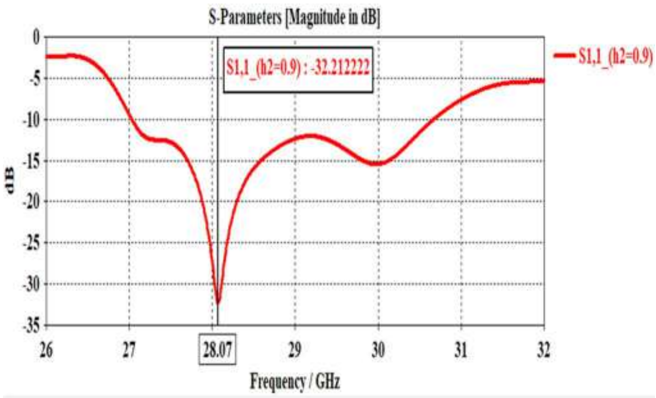

Figure 9: Return Loss of Antenna 02

The analysis of the impedance bandwidth, as depicted on the S11 plot of Antenna 02, is noted in Figure 10. With the (-10 dB) as a criterion of acceptable performance, the Antenna has a return loss of below -10 dB between 27.429 GHz and 30.779 GHz. This comes with a large operation bandwidth of 3.3498 GHz. The wide bandwidth implies that Antenna 02 can maintain strong connections and transmit high data rates, enabling it to distribute less error

Int. J. Advanced Networking and Applications
Volume: 17 Issue: 04 Pages: 7008-7022 (2025) ISSN: 0975-0290
DOI :

prone communications over a vast range of frequencies that is particularly useful in 5G systems, especially in millimeter- wave applications. The high level of both return loss and bandwidth confirms that the antenna exhibits effective overall performance in terms of being broadband.

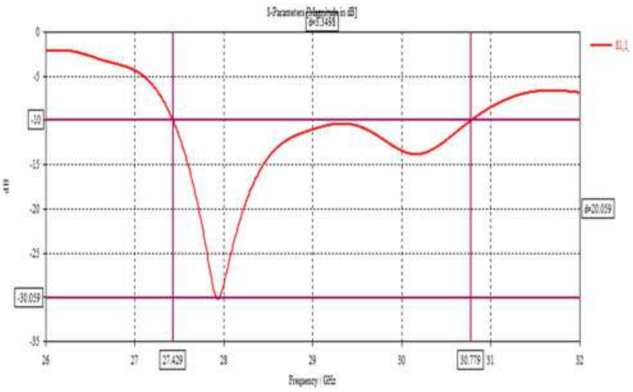

Figure 10: Graphical Analysis of Bandwidth of Antenna 02

$S11$ properties of the antenna are illustrated in Figure 11, spanning a frequency range of 26 GHz to 32 GHz. In the plot, a sharp resonance is observed at a frequency of around 28 GHz, where the return loss is below -25 dB, indicating that this frequency exhibits excellent impedance matching in the network. Consequently, any power passing through the network at this frequency will be reflected with minimal loss. Additionally, the return loss is inferior, by far, to -10 dB over a wide frequency range, indicating good performance over a broad band. This action demonstrates that the antenna is adequately optimized to operate at millimeter waves and is highly suitable for 5G and other high- frequency wireless communications systems that require wide bandwidths and effective power delivery.

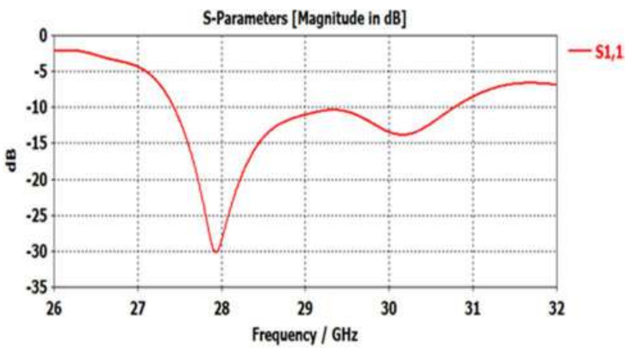

Figure 11: Graphical representation of the S_{11} reflection coefficient for the antenna, showing the measured results and adaptation at the resonant frequency.

Now it is time to change the resonating frequency of the antenna, and at present the frequency is 28 GHz. Based on the comparison of various results following manipulation of values, including the length of the substrate, L1, and width, W, some linear associations have been found that will help increase the bandwidth and return loss, thereby changing the resonating frequency to 28 GHz. The first advantage that these changes brought was an increase in return loss, as they led to a better impedance match, which is crucial for the effective transfer of power. That alteration enabled the antenna to perform more efficiently at the desired frequency, and it transmitted fewer signals to be reflected, thereby increasing its efficiency. The length and width of the substrate were chosen to match the resonating frequency at 28 GHz, which plays a critical role in meeting the peculiarities of the 5G communication network. As Figure 22 depicts, it may be observed that by adjusting values of both the variables, namely, "L1" and "W, a linear correlation has been established which also aids in optimizing the performance of the antenna. Specifically, by varying the value of h2 through parametric sweep command, observers can observe the resonant frequency spike approaching a 28 GHz frequency. This is the tuning process, which shows us that fine-tuning of these helps to get along, trying to achieve the suitable resonating frequency as well.

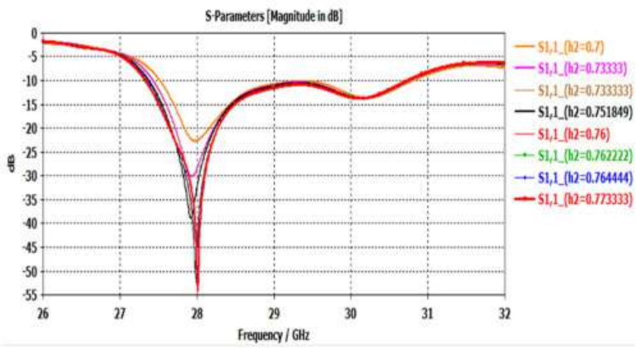

Figure 12: Sweep Command Results of Antenna 02

The calculation of the bandwidth of Antenna 02 is displayed in Figure 13, which is determined using the S11 parameter. The reference point is at -10 dB, and the acceptable impedance region begins at this point. The graph suggests that the antenna has a total impedance bandwidth of 3.3989 GHz, maintaining a return loss of less than -10 dB between approximately 27.33 GHz and 30.729 GHz. Such a broad bandwidth proves that Antenna 02 is indeed the best candidate for broadband millimeter-wave applications (at 28 GHz, as used in 5G systems). The high null at resonance (-54.129 dB) further demonstrates good impedance matching and a very low reflected signal, indicating the efficiency and strength of the constructed antenna.

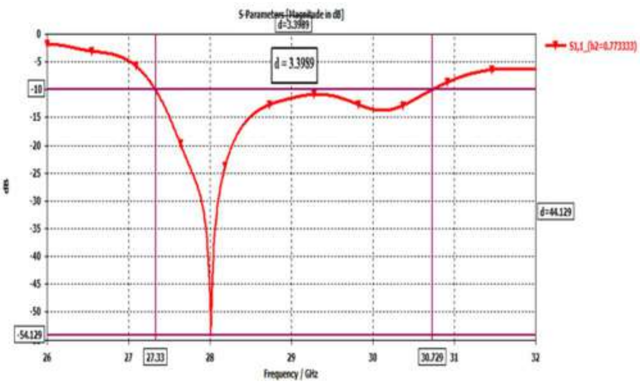

Figure 13: Bandwidth Calculation of Antenna 02

Volume: 17 Issue: 04 Pages: 7008-7022 (2025) ISSN: 0975-0290
DOI :

The $S11$The calculation provided in Figure 14 indicates that Antenna 02 is resonant at 28.01 GHz. The minimum value of return loss at this frequency is -54.129 dB, indicating good impedance matching and extremely low signal reflection. The low-loss null ensures efficient power transfer from the feed line to the antenna, a crucial consideration for high-performance millimeter-wave systems. The broad return loss curve indicates that the antenna has a broadband match, providing good matching over a wide frequency range, which is a key strength of the antenna that qualifies it for use in broadband applications, such as 5 G. This outcome confirms the strength of design and effectiveness of the antenna at the intended frequency.

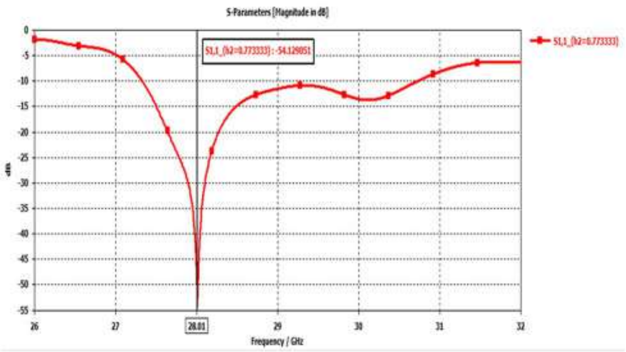

Figure 14: Return Loss Calculation of Antenna 02

The parameters are crucial in determining the efficiency of the antenna, specifically in terms of radiation efficiency and total efficiency, which measure how well the antenna converts input power into emitted radiated electromagnetic waves. Higher radiation efficiency means that a large portion of the input power is successfully radiated. In contrast, total efficiency reflects radiation losses as well as losses due to material and design inefficiencies. These efficiencies have a direct impact on the antenna's performance and its practical applicability. Figure 15 illustrates the efficiency performance of Antenna 02 at 28 GHz, presenting both radiation efficiency and total efficiency. The radiation efficiency is measured at approximately –1.086 dB. Using the relation $\eta = 10^{\frac{Efficiency\ (dB)}{10}}$, this corresponds to a linear efficiency of about 78.4%. This result indicates that most of the input power is effectively converted into radiated electromagnetic waves, with only minor losses attributed to conductor and dielectric properties. Similarly, the total efficiency is also recorded at –1.086 dB, yielding the same linear efficiency of approximately 78.4%. The close correspondence between radiation and total efficiencies demonstrates excellent impedance matching and minimal reflection losses. Such high efficiency confirms the optimized design of Antenna 02, ensuring reliable radiative performance at millimeter-wave frequencies. These results highlight the antenna’s suitability for modern 5G and beyond communication systems, where high transmission efficiency and minimal energy loss are essential for robust and energy-efficient operation.

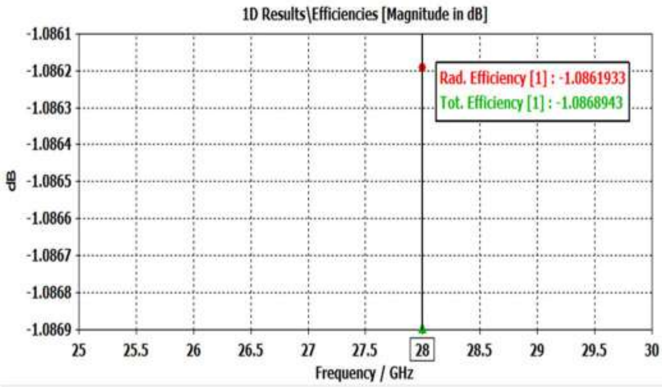

Figure 15: Radiation and Total Efficiency of Antenna 02

In directivity, this is the parameter that shows how much the antenna concentrates energy as a beam into a specific direction; this is a very important parameter for maximizing communication levels and reducing interferences. The directivity of the antenna provides insight into the antenna's ability to direct its radiated power in a specific direction, thereby enhancing overall performance, particularly in cases where the system requires focused high-power radiation. We have the 3D radiation pattern of the directivity of Antenna 02 at 28 GHz, in Figure 16. Under all conditions, the antenna achieves a peak directivity of 7.703 dBi, and the direction of radiation indicates that the main lobe is primarily directed along the x-axis. The radiation pattern suggests the existence of a well-developed principal lobe and relatively suppressed side lobes, indicating good directional characteristics. The radiation and total efficiencies are both measured to be equal to -1.08 dB, which means minimal power loss and efficient radiation. The high efficiency of this directivity level also shows the ability of the antenna to transmit focused energy and would be an excellent choice of antenna in high-frequency, directional communication systems such as the 5G and MM Wave radar applications.

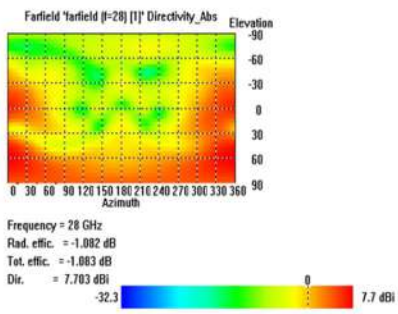

Figure 16: 2-D Visualization of Antenna 02 Directivity

Figure 17 indicates the 2-D polar chart of the normal radiation of Antenna 02 at 28 GHz in the Phi = 90 ° plane. The antenna has a main lobe of 4.2 dBi at an angle of 86°, which is a strong and directed radiation that is offset from the broad side. The angular width of the beam is 62 degrees at the 3 dB level, resulting in a quite narrow and directional pattern. The level of side lobes is set at -5.2 dB, indicating moderate suppression of unwanted wave

Volume: 17 Issue: 04 Pages: 7008-7022 (2025) ISSN: 0975-0290
DOI :

directions. This result suggests that the antenna is certain to be applicable in directional and beam-steered tasks, including *mm* Wave 5G, where the focused transmission and impeded interference are vital.

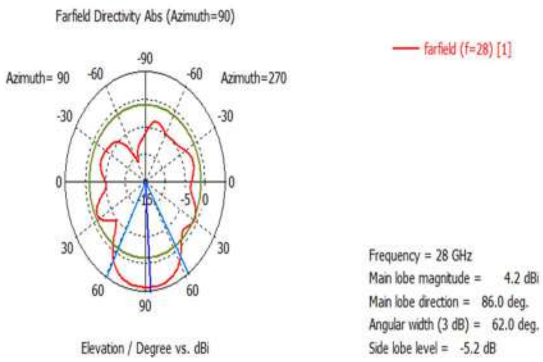

Figure 17: Polar Graphical View of Directivity

Table 4 shows the detailed design parameters used for Antenna 02, including geometric dimensions and material properties. The antenna is built on a dielectric substrate with a relative permittivity (εr) of 2.20, a substrate height of 0.79*mm*, and a width of 9.72346 *mm*, all contributing to low-loss performance at millimeter-wave frequencies. Key structural parameters—such as lengths L = 13 *mm*, Lsiw = 8 mm, and widths W = 9.72346 *mm*, Wsiw = 9.60 *mm* Suggest the use of substrate-integrated waveguide (SIW) features, which improve guided wave propagation and impedance matching. The trace dimensions, including a width of 2.8 mm and a thickness of 0 *mm*, reflect a microstrip or etched metal configuration. The fine-tuned dimensions across various slots and feed structures (e.g., Ls1 = 0.2 *mm*, Strp = 0.035 *mm*). They are carefully optimized to achieve resonance at approximately 28 GHz. This precise parameterization ensures efficient operation, a broad bandwidth, and strong radiation performance, making it suitable for 5G and other advanced wireless systems.

Table 4: Antenna 02 Design Parameters

Parameter	*Dimension*	*Parameter*	*Dimension*
L	13.0mm	L6	8.5mm
L1	11.6mm	Ls1	0.2mm
L2	4.8mm	Ls2	1.0mm
L3	9.0mm	Lsiw	8.0mm
L4	7.3mm	Strp	0.035mm
L5	1.0mm	H	0.79mm
W2	3.0mm	W1	2.454mm
W4	3.6mm	W3	9.0mm
W5	1.6mm	Wsiw	9.6mm
W6	0.25mm		

4.3 Modified Cavity Patch Antenna

Figure 18 shows the structural layout of the proposed cavity patch antenna, divided into two main views: (a) the upper patch view and (b) the lower patch view. In Figure 18(a), the upper patch view presents a symmetrical radiating structure with various slots and rectangular segments engineered for enhanced bandwidth and resonance stability at millimeter-wave frequencies. The central feed line and precisely dimensioned cutouts help achieve effective impedance matching and mode confinement. Figure 28(b) shows the lower patch view, incorporating SIW slots and periodic via holes along the edges to form a well-defined cavity. These SIW features support-controlled wave propagation, reduced surface wave losses, and improved directivity. The combined multilayer structure of the upper and lower patches forms a compact, high-efficiency antenna suitable for 5G and other applications. *mm*Wave applications.

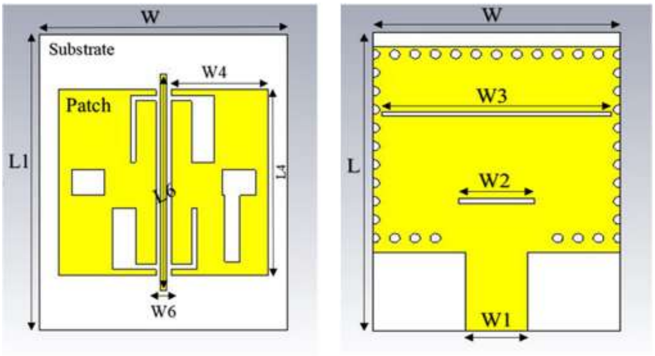

(a) (b)

Figure 18: Structure of proposed cavity patch antenna (a) proposed antenna upper patch view (b) proposed antenna lower patch view.

Table 5 presents the optimized physical dimensions of the proposed dual-beam cavity-backed patch antenna, designed for operation in the millimeter-wave band. The parameters include critical structural values such as widths, lengths, and slot and spacing elements. These parameters are specifically adjusted to achieve the optimal match of impedance, a wide bandwidth, and dual radiation beams. The combination of SIW cavity dimensions results in good wave confinement and minimization of surface wave losses. The selected height of substrate h = 0.79 *mm* strikes a good balance between mechanical stability and high-frequency performance, meeting the compact and efficient requirements of 5G communication systems.

Table 5: Optimize dimensions of dual-beam cavity-backed patch antenna

Parameter	*Dimension*	*Parameter*	*Dimension*
L	15.8mm	L6	7.5mm
L1	12.8mm	Ls1	0.2mm
L2	4.8mm	Ls2	1.0mm
L3	9.0mm	Lsiw	8.0mm
L4	7.3mm	Strp	0.035mm
L5	1.0mm	H	0.79mm
W2	4.7mm	W1	2.6mm
W4	3.6mm	W3	9.0mm
W5	1.6mm	Wsiw	9.6mm
W6	0.4mm	H	0.77mm

Volume: 17 Issue: 04 Pages: 7008-7022 (2025) ISSN: 0975-0290
DOI :

Table 6 shows the optimized design parameters for the proposed Antenna-3, a high-performance cavity-backed patch antenna intended for millimeter-wave applications. The table includes precise geometric values critical to achieving the desired dual-beam radiation characteristics. Notable parameters include slot and patch widths, as well as key structural lengths. Slot spacing and cavity configurations are also defined, enabling precise impedance matching and wave confinement. The via spacing (Svp = 0.8), pin hole diameter (Ph = 0.035), and substrate height (h= 0.79mm) contribute to maintaining high radiation efficiency and structural integrity. These carefully tuned dimensions validate the antenna's performance in wideband and directional communication environments, especially for 5G and next-generation $mmWave$ systems.

Table 6: Optimize dimensions of proposed antenna

Parameter	***Dimension***	***Parameter***	***Dimension***
L	13mm	L6	7.5mm
L1	12.8mm	Ls1	0.2mm
L2	4.8mm	Ls2	1.0mm
L3	9.0mm	Lsiw	8.0mm
L4	7.3mm	Strp	0.035mm
L5	1.0mm	H	0.79mm
W2	3.0mm	W1	2.454mm
W4	3.6mm	W3	9.0mm
W5	1.6mm	Wsiw	9.6mm
W6	0.25mm	h_2	0.77mm

Figure 19 shows the simulated S-parameter S11 response of the proposed antenna over the frequency range of 26–32 GHz. The results demonstrate excellent impedance matching exactly at the resonant frequency of 28.01 GHz, where the return loss reaches a value of –54.129 dB, indicating near-total power absorption with minimal reflection. Additional simulations for varying configurations or parameter sets show return losses of -50.53638 dB and -51.5000 dB, respectively, further confirming the antenna's robustness and stability across minor design variations. All curves maintain return loss levels well below –10 dB over a broad bandwidth, validating the antenna's efficiency and wideband operation. This performance highlights the proposed antenna's suitability for millimeter-wave applications.

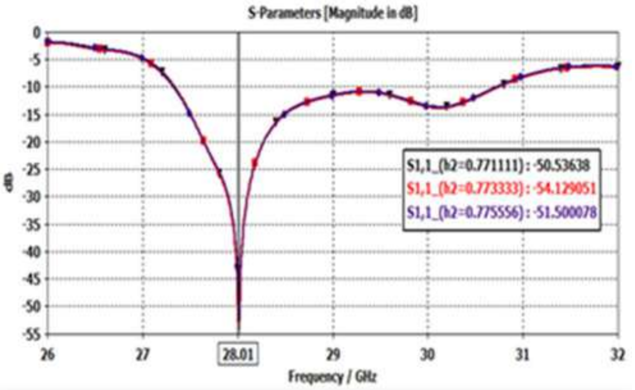

Figure 19: S parameter of the proposed antenna

Figure 20 illustrates the simulated VSWR of the proposed cavity patch antenna within the 26–32 GHz band. At the resonant frequency of 28 GHz, the antenna exhibits a VSWR of 1.0078, which is nearly identical to the ideal value of unity, confirming excellent impedance matching with negligible reflection. Moreover, the VSWR remains below 2 across the entire operating band, indicating stable broadband behavior. These results verify the high efficiency of the proposed design and its suitability for millimeter-wave applications such as 5G and beyond communication systems.

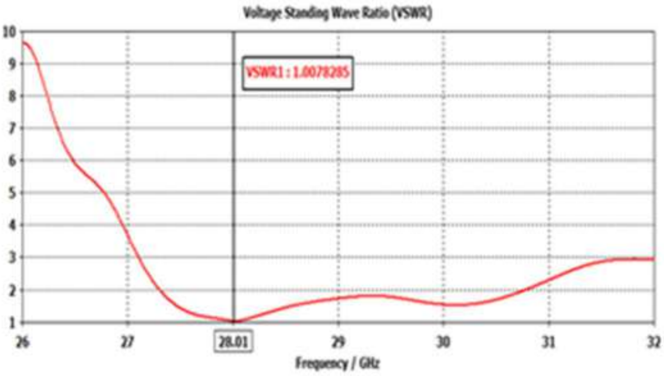

Figure 20: VSWR of the proposed cavity patch antenna

5. DISCUSSION

Table 7: Proposed vs Existing Model

Parameter	**Proposed Model**	**Existing Model**
Operating Frequency	26–32 GHz	27.8–30.9 GHz
Bandwidth	3.3989 GHz (~12.1% FBW)	~3.1 GHz (~10.6% FBW)
Return Loss	-54.13 dB	< -10 dB
Directivity	7.708 dBi	~8.5 dBi
Radiation Efficiency	~78%	Not reported
Total Efficiency	~78%	Not reported
Polarization	Linear	Linear
Number of Beams	Dual-beam	Dual-beam
Beam Direction	0° and ~86°	±47°

The proposed cavity-backed microstrip antenna, designed for the 28 GHz near-millimeter wave band, demonstrates excellent performance enhancements through successive design refinements. Starting with a basic patch antenna, improvements were made through the inclusion of a substrate-integrated waveguide (SIW) feed, followed by U- and L-shaped cavity cuts, and ultimately, a hammer-shaped slot, resulting in significant improvements in impedance matching and bandwidth. Among the three designs modeled in CST Microwave Studio, Antenna #03 showed the most promising results, achieving an

Volume: 17 Issue: 04 Pages: 7008-7022 (2025) ISSN: 0975-0290
DOI :

impressive return loss of –54.12904 dB and a wide fractional bandwidth of ~12.1% (3.3989 GHz), while maintaining a moderate gain of approximately 6.63 dBi and a directivity of about 7.708 dBi. These results exceed the –10 dB $|S_{11}|$ benchmark, indicating a highly efficient energy transfer from the feed to the radiating element. A parametric analysis by varying the patch height shall further unveil its influence on the antenna performance and size. Increasing the patch height above 0.035 mm increases the impedance bandwidth from 3.3989 GHz to 3.466 GHz due to strong fringing fields but degrades the magnitude of return loss from -54.13 dB to -43.507 dB, hence showing reduced impedance matching, apart from that fact that radiation efficiency and total efficiency remain almost the same and directivity slightly reduces from 7.708 dBi to 7.298 dBi, a patch height of 0.035 mm has been chosen as an optimal design choice offering a balanced trade-off between bandwidth enhancement and impedance matching together with radiation characteristics for the proposed 28GHz antenna.

The observed performance gains are primarily attributed to the integration of the SIW cavity structure, which helps suppress surface-wave leakage and concentrates the electromagnetic energy beneath the patch. Additionally, the L-shaped and hammer-shaped cuts introduced in the cavity increased the effective current path, allowing for the excitation of multiple resonant modes and consequently broadening the impedance bandwidth. These findings align with prior SIW-based studies, which have noted similar bandwidth expansions resulting from effective current redistribution at the edges of the patch. However, the exceptionally low return loss recorded in this study indicates improved matching conditions between the feed and the radiating structure compared to previously reported designs. When compared with related works summarized in the manuscript, the proposed antenna stands out due to its compact size and superior bandwidth. Most of the comparable single-element 5G antenna designs report bandwidths in the 2–8% range. In contrast, the ~12.1% bandwidth achieved here, combined with a small footprint of just 13 mm ×9.72346 mm surpasses many multilayer and LTCC-based counterparts in terms of practical applicability. While some 60 GHz designs achieve higher gains, they often come at the cost of increased complexity and fabrication challenges. The proposed design, therefore, represents a practical balance between performance, simplicity, and manufacturability, especially for use in compact 5G devices such as handsets or small-cell nodes.

The strong return loss of better than –20 dB across the 26–32 GHz range makes the design highly suitable for real-world 5G applications, as it reduces dependence on complex matching networks in RF front-end modules. The bandwidth also supports full coverage of 3GPP's n257 and n258 bands, facilitating multi-operator or aggregated-carrier deployments with a single antenna unit. Additionally, the dual-beam radiation pattern observed suggests potential for basic beam steering in access points without requiring mechanical adjustments—an important consideration for fixed-wireless access systems.

Despite these promising results, this work is limited to simulation-based analysis. Practical challenges, such as precise fabrication of the Rogers RT5880 substrate with a thickness of 0.79mm, may introduce alignment errors in the SIW vias. These issues, along with potential surface roughness losses at 28 GHz and thermal effects, may reduce the actual performance compared to simulations. Also, integration with RF components and system-level effects like coupling in multi-element arrays were not considered in this study.

Future work should address these limitations through physical prototyping and experimental validation using S-parameter and radiation pattern measurements. Scaling up the design into phased array configurations, evaluating dual-polarization options, and co-designing with RF front ends will help bring the concept closer to real-world deployment. Such developments could ultimately enable compact, high-performance 5G antenna modules suitable for gigabit-class connectivity in dense urban environments.

6. CONCLUSIONS

In this paper, we have provided a cavity patch antenna that is compatible with 5 G wireless communication. The antenna consists of a substrate-integrated waveguide (SIW) cavity that operates in a symmetrical patch along y-axis. The symmetrical patch is fed by the SIW cavity and works at quasi-TM 20 mode whereas the SIW cavity works at TM 12 0 mode. The simulation shows the antenna being proposed has a bandwidth between 26 -32 GHz with the resonant frequency at 28 GHz, and the fractional bandwidth of 11.71%. Limiting antenna structure design, impedance bandwidth could be extended nearly 3.3989 GHz and the level of return loss was enhanced to -54.129dB at the resonating frequency. Besides, some parts of the antenna were reduced in size in a great deal, and the whole assembly was simplified to be practically manufacturable which guarantees affordability in cost and ease of implementation in the wireless systems later. The findings describe the capacity of the antenna to be used at a high frequency hence very useful in next generation 5G applications. Experiments also show that the antenna size reduction, enhancement of performances, and optimization of parameters can be improved more and this possibility can be pursued in future communication networks. The current work clears the path towards the future compact presents and efficient designs of antennas that are capable of sustaining the challenging needs of 5G and beyond, specifically in high-data-rate, minimum latency schemes.

Data Availability: All relevant data are within the manuscript. The collection and analysis method complied with the terms and conditions for the source of the data.

Volume: 17 Issue: 04 Pages: 7008-7022 (2025) ISSN: 0975-0290
DOI :

Funding: This research received no specific grant from any funding agency in the public, commercial, or not-for-profit sectors.

Author Contributions: Kalim Ullah, Wajid Khan: Conceptualization, Methodology, Software, Visualization, Investigation, Writing- Original draft preparation. Abdul Aziz, Mubarak Zeb, Muhammad Zain Yousaf: Data curation, Validation, Supervision, Resources, Writing - Review & Editing. Muneera Altayeb, Viktoriia Bereznychenko: Project administration, Supervision, Resources, Writing - Review & Editing.

Conflicts of Interest: The authors stated that no conflict of Interest.

REFERENCES

[1] Ullah, Habib, et al. "Angularly Stable Band Stop FSS Loaded MIMO Antenna with Enhanced Gain and Low Mutual Coupling." Int. J. Advanced Networking and Applications 15.03 (2023): 5924-5930.

[2] Andrews, J.G., Buzzi, S., Choi, W., et al.: ‘What will 5G be?’, IEEE J. Sel. Areas Commun., 2014, 32, (6), pp. 1065–1082

[3] Rappaport, T., Sun, S., Mayzus, R., et al.: ‘Millimeter wave mobile communications for 5G cellular: It will work! IEEE Access, 2013, 1, pp. 335–349.

[4] Sulyman, A.I., Nassar, A.T., Samimi, M.K., et al.: ‘Radio propagation path loss models for 5G cellular networks in the 28 and 38 GHZ millimeter-wave bands’, IEEE Commun. Mag., 2014, 52, (9), pp. 78–86

[5] Hong, W., Baek, K.-H., Lee, Y., et al.: ‘Study and prototyping of practically large-scale mmwave antenna systems for 5G cellular devices’, IEEE Commun. Mag., 2014, 52, (9), pp. 63–69

[6] Boccardi, F., Heath, R.W., Lozano, A., et al.: ‘Five disruptive technology directions for 5G’, IEEE Commun. Mag., 2014, 52, (2), pp. 74–80

[7] Hong, W, Jiang Z, H, Yu, C, et al.: ‘Multibeam antenna technologies for 5G wireless communications’, IEEE Trans. Antennas Propag., 2017, 65, (12), pp. 6231–6249

[8] L. Wang, Y.-X. Guo, and W.-X. Sheng, “Wideband high-gain 60-GHz LTCC L-probe patch antenna array with a soft surface,” IEEE Trans. Antennas Propag., vol. 61, no. 4, pp. 1802–1809, Apr. 2013

[9] W. M. Abdel-Wahab, and S. Safavi-Naeini. “Wide-Bandwidth 60-GHz Aperture-Coupled Microstrip Patch Antennas (MPAs) Fed by Substrate Integrated Waveguide (SIW),” IEEE Antennas Wireless Propag. Lett.vol. 10, pp. 1003-1005, 2011.

[10] Y.-X. Guo and H. Chu, “60-GHz LTCC dielectric resonator antenna array,” in Proc. IEEE APS, Orlando, FL, USA, Jul. 2013,pp. 1874–1875.

[11] T. H. Jang, H. Y. Kim, I. S. Song, C. J. Lee, J. H. Lee, and C. S. Park, “A wideband aperture efficient 60-GHz series-fed Eshaped patch antenna array with copolarized parasitic patches,” IEEE Trans. Antennas Propag., vol. 64, no. 12, pp. 5518–5521, Dec. 2016

[12] N. C. Karmakar, “Investigations into a cavity-backed circular-patch antenna,”IEEE Trans. Antennas Propag., vol. 50, no. 12, pp. 1706–1715,Dec. 2002.

[13] J. T. Aberle, “On the use of metallized cavities backing microstrip antennas,” in Proc. IEEE AP-S Int. Symp. Dig., pp. 60–63, 1993.

[14] M. M. Honari, R. Mirzavand, H. Saghlatoon, and P. Mousavi, “A dualband low-profile aperture antenna with substrate-integrated waveguide grooves,” IEEE Trans. Antennas Propag., vol. 64, no. 4, pp. 1561–1566, Apr. 2016.

[15] W. Yang and J. Zhou, “Wideband low-profile substrate integrated waveguide cavity-backed E-shaped patch antenna,” IEEE Antennas Wireless Propag. Lett., vol. 12, pp. 143–146, Jan. 2013.

[16] K.-S. Chin et al., “Wideband LTCC 60-GHz antenna array with a dual-resonant slot and patch structure,” IEEE Trans. Antennas Propag., vol. 62, no. 1, pp. 174–182, Jan. 2014.

[17] Y. Zhang, Z. N. Chen, X. Qing, and W. Hong, “Wideband millimeter-wave substrate integrated waveguide slotted narrow-wall fed cavity antennas,” IEEE Trans. Antennas Propag., vol. 59, no. 5, pp. 1488–1496, May 2011.

[18] G. Q. Luo, Z. F. Hu, L. X. Dong, and L. L. Sun, “Planar slot antenna backed by substrate integrated waveguide cavity,” IEEE Antennas Wireless Propag. Lett. vol. 7, pp. 236–239, 2008.

[19] W. Han, F. Yang, J. Ouyang and P. Yang, “Low-cost wideband and high-gain slotted cavity antenna using high-order modes for millimeter-wave application,” IEEE Trans. Antennas Propag., vol. 63, no. 11, pp. 4624-4631, Nov. 2015.

[20] W. Li, K. D. Xu, X. Tang, Y. Yang, Y. Liu and Q. H. Liu, "Substrate Integrated Waveguide Cavity-Backed Slot Array Antenna Using High- Order Radiation Modes for Dual-Band Applications in K-Band," IEEE Trans. Antennas Propag., vol. 65, no. 9, pp. 4556-4565, Sept. 2017.

[21] K. Gong, Z. Chen, X. Qing, P. Chen, and W. Hong, “Substrate integrated waveguide cavity-backed wide slot antenna for 60-GHz bands,” IEEE Trans. Antennas Propag., vol. 60, no. 12, pp. 6023–6026, Dec. 2012.

Volume: 17 Issue: 04 Pages: 7008-7022 (2025) ISSN: 0975-0290
DOI :

[22] Q. Zhu, K. B. Ng, C. H. Chan and K. M. Luk, "Substrate-Integrated-Waveguide-Fed Array Antenna Covering 57–71 GHz Band for 5G Applications," IEEE Trans. Antennas Propag., vol. 65, no. 12, pp. 6298-6306, Dec. 2017.

[23] K. Fan, Z. C. Hao and Q. Yuan, "A Low-Profile Wideband Substrate-Integrated Waveguide Cavity-Backed E-Shaped Patch Antenna for the Q-LINKPAN Applications," IEEE Trans. Antennas Propag., vol. 65, no. 11, pp. 5667-5676, Nov. 2017.

[24] T. Y. Yanget al., "Wideband millimeter-wave substrate integrated waveguide cavity-backed rectangular patch antenna," IEEE Antennas Wireless Propag., Lett.vol.13, pp. 205–208, 2014.

[25] Y. J. Li and K. M. Luk, "Low-cost high-gain and broadband substrate integrated waveguide fed patch antenna array for 60-GHz band," IEEE Trans. Antennas Propag., vol. 62, no. 11, pp. 5531–5538, Nov. 2014.

[26] Y. Li and K.-M. Luk, "60-GHz substrate integrated waveguide fed cavity-backed aperture-coupled microstrip patch antenna arrays," IEEE Trans. Antennas Propag., vol. 63, no. 3, pp. 1075–1085, Mar. 2015

[27] G. Q. Luo, Z. F. Hu, L. X. Dong, and L. L. Sun, "Planar slot antenna backed by substrate integrated waveguide cavity," IEEE Antennas Wireless Propag. Lett., vol. 7, pp. 236–239, 2008.

[28] W. Han, F. Yang, J. Ouyang and P. Yang, "Low-cost wideband and high-gain slotted cavity antenna using high-order modes for millimeter- wave application," IEEE Trans. Antennas Propag., vol. 63, no. 11, pp. 4624-4631, Nov. 2015.

[29] W. Li, K. D. Xu, X. Tang, Y. Yang, Y. Liu and Q. H. Liu, "Substrate Integrated Waveguide Cavity-Backed Slot Array Antenna Using High-Order Radiation Modes for Dual-Band Applications in K-Band," IEEE Trans. Antennas Propag., vol. 65, no. 9, pp. 4556-4565, Sept. 2017.

[30] K. Gong, Z. Chen, X. Qing, P. Chen, and W. Hong, "Substrate integrated waveguide cavity-backed wide slot antenna for 60-GHz bands," IEEE Trans. Antennas Propag., vol. 60, no. 12, pp. 6023–6026, Dec. 2012.

[31] Q. Zhu, K. B. Ng, C. H. Chan and K. M. Luk, "Substrate-Integrated-Waveguide-Fed Array Antenna Covering 57–71 GHz Band for 5G Applications," IEEE Trans. Antennas Propag., vol. 65, no. 12, pp. 6298-6306, Dec. 2017.

[32] R. Garg, P. Bhartia, I. Bahl, and A. Ittipiboon, Microstrip Antenna Design Handbook. Norwood, MA, USA: Artech House, 2001.

[33] V. Sharma, "Analysis of Microstrip Patch Antenna using Transmission Line Model," Int. J. Adv. Ind. Res., Feb. 2014.

[34] P. Banerjee and T. Bezboruah, "Comparative Study of Transmission Line and Cavity Model of Rectangular Microstrip Antenna," Int. J. Nat. Sci. Res., vol. 3, no. 6, pp. 76-82, 2015.

[35] Y. T. Lo, D. Solomon, and W. F. Richards, "Theory and Experiment on Microstrip Antennas," IEEE Trans. Antennas Propag., vol. 27, no. 2, pp. 137-145, Mar. 1979.

Author Biography:

1. **Kalim Ullah** holds a BSc in **Electrical Engineering (Communication)** from the University of Engineering and Technology, Peshawar, Pakistan, and a Master's degree in **Mathematics** from the University of Lakki Marwat. He has three years of professional experience in the electrical engineering sector. His research interests include 5G and 6G wireless communication systems, antenna design, and the integration of artificial intelligence in next-generation communication technologies.

2. **Abdul Aziz** is a PhD student at Tianjin University, China, specializing in Microgrid Systems. His current research focuses on the development of Lunar Microgrid technologies. He holds a Bachelor's degree in Electrical Engineering from the University of Engineering and Technology (UET) Peshawar and a Master's degree from CECOS University of IT and Emerging Sciences, Peshawar.

3. **Mubarak Zeb** completed his BSc in Electrical and Computer Engineering from the International Islamic University Islamabad, Pakistan. His areas of academic interest include electrical and computer engineering, emerging communication technologies, and applied research in modern engineering systems.